Pergamon

Building and Environment, Vol. 32, No. 4, pp. 3
© 1997 Elsevier Science Ltd. All ri
Printed in
0360–1323/97

10658

PII: S0360–1323(97)00002–4

Using Computational Fluid Dynamics as a Design Tool for Naturally Ventilated Buildings

M. J. CLIFFORD*
P. J. EVERITT†
R. CLARKE†
S. B. RIFFAT†

(*Received* 19 *August* 1996; *revised* 21 *October* 1996; *accepted* 28 *November* 1996)

Results from testing of a simple model in a wind tunnel are used to validate two computational fluid dynamics mathematical models. The results show that only the Reynolds-stress model provides a reasonably accurate representation of the internal flow, and that both models fail to predict the flow at the opening of the model. © 1997 *Elsevier Science Ltd.*

INTRODUCTION

Natural ventilation has been utilised for many years as the major process to provide fresh air and indoor air movement for thermal comfort in buildings. However, estimating the quantity of ventilation for any particular building at the design stage is still a difficult task. Until recently, the preferred method was to build a scale model and test the model in a wind tunnel. Developments in wind tunnel techniques such as boundary layer simulation and improvements in modelling wind characteristics have lead to reasonable estimates of ventilation rates, but other factors such as complex topographic features, scaling errors, and influence of architectural features can restrict the accuracy of any estimate [1–4]. An alternative approach is to apply the mathematical modelling technique of computational fluid dynamics (CFD) [5]. This has many attractions: there is no need to build a physical model, different wind characteristics (e.g. turbulence) are easy to simulate, and detailed results can be obtained where it may be difficult to take measurements from a scale model. These advantages have led to a large number of simulations of buildings with various features [6, 7]. Internal air flow inside buildings has also been modelled, even allowing for obstructions to the flow such as furniture and people [8]. It is easy to produce a detailed picture of the air flow with little computational effort. However, the application of CFD without reference to model testing should be avoided since there is no guarantee that the predicted air flow is a true representation. In this paper we show that even for the simplest geometry, CFD can give misleading results which dramatically affect the predicted ventilation rate.

*Department of Theoretical Mechanics, University of Nottingham, University Park, Nottingham NG7 2RD, U.K.
†Institute of Building Technology, Department of Architecture and Building Technology, University of Nottingham, University Park, Nottingham NG7 2RD, U.K.

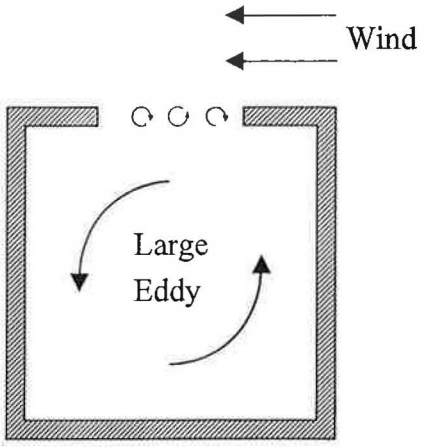

Fig. 1. Single-sided ventilation.

In the following we consider the situation depicted in Fig. 1: the flow past a square opening in a cube, an archetype of single-sided ventilation. The flow is perpendicular to the opening, and air exchange occurs via infiltration. Also note the large eddy which forms inside the cube. This could be a very crude representation of the flow past an open window. Here we combine wind tunnel testing with CFD to test the validity of the mathematical model.

EXPERIMENTAL PROCEDURE

Wind tunnel testing

The tunnel used for this series of tests was based on a small open-jet wind tunnel developed for teaching purposes by the Building Research Establishment. This tunnel has a maximum flow rate of 4.5 m/s and a working section 1.0 m wide by 0.75 m high and 2.25 m long. For the purpose of this experiment, the wind speed is maintained at 3 m/s throughout. Two layers of honeycomb

are fitted in the bellmouth to straighten the incoming flow, and are followed by a 0.5 mm mesh screen. Beyond the entry section there is a 0.75 m settling chamber to allow disturbances caused by the honeycomb and screen to decay, and to allow means to be introduced to modify the flow profile. A transformer is positioned between the working section and the fan to convert the 1.0 m × 0.75 m cross-section to a suitable shape for the fan mounting. The entry to the transformer is larger than the settling chamber exit in order to allow for some expansion of the flow through the working section.

The tunnel was measured to determine any velocity variations across the tunnel section. Two sets of data were recorded: the first measured 0.5 m downstream of the settling chamber, and the second a further 1 m downstream. Only negligible velocity variations were found (±3%), although the turbulence intensity was higher at the second location. The flow through the tunnel was found to be stable up to 0.2 m from the edge of the table.

A box constructed of medium-density fibreboard measuring 0.5 m × 0.5 m × 0.5 m, with a 0.25 m square opening in the centre on one side, was set into the wind tunnel table. The box had holes drilled in one side to allow for the insertion of an air velocity transducer. The air velocity transducer used was omnidirectional, and had a response time of 0.2 s. Readings of air speed from the probe were averaged over 30 s. For the purpose of these experiments, wind tunnel speed was set to 3 m/s throughout.

Computational fluid dynamics

In this investigation the CFD package FLUENT V4.2.5 was used for all numerical simulations. FLUENT V4.2.5 comes in two sections. The first, preBFC, is a CAD-type package, and allows detailed geometries to be entered to produce a true representation of the experimental set-up. It also employs body-fitted coordinates, which facilitates mapping of the grid. The second sect is FLUENT itself. In this section all the physical c stants and boundary conditions are entered, and the c rect models are activated. FLUENT is the main sect of this package and is where the fluid dynamics equati are solved.

The flow under investigation is a 3D, steady-st incompressible, turbulent flow. Two different turbul models were tried: the k–ϵ model and the Reynolds-st model. Although the fluid used is air, it can be conside incompressible due to the relatively low flow rates u Gravitational force was also calculated in the final s tion.

The computational grid used for both simulati shown in Fig. 2, had 50 cells in the x-direction responding to the direction down the tunnel, 25 cell the z-direction across the tunnel, and 40 cells in the v cal, y-direction, a total of 50 000 cells. The grid was n uniform, and grid lines were concentrated after the op ing, and inside the box to give an accurate representat of the internal flows. The large upstream distance chosen to allow the flow to settle before the opening, also to model the wind tunnel dimensions. The res were checked by doubling the number of cells in e direction for a few cases, which gave compar results.

In the FLUENT User Guide [9], the calculation cedure uses the conventional equations adapted f the conservation and Navier–Stokes equations. To m them relevant for turbulent flow, the equation set is cl via the Reynolds time averaging procedure and the closure model. The k–ϵ turbulence model is an eddy cosity model in which the Reynolds stresses are assu to be proportional to the mean velocity gradients, the constant of proportionality being the turbulent e viscosity, μ_t. This assumption, known as the Boussi hypothesis, provides the following expression for

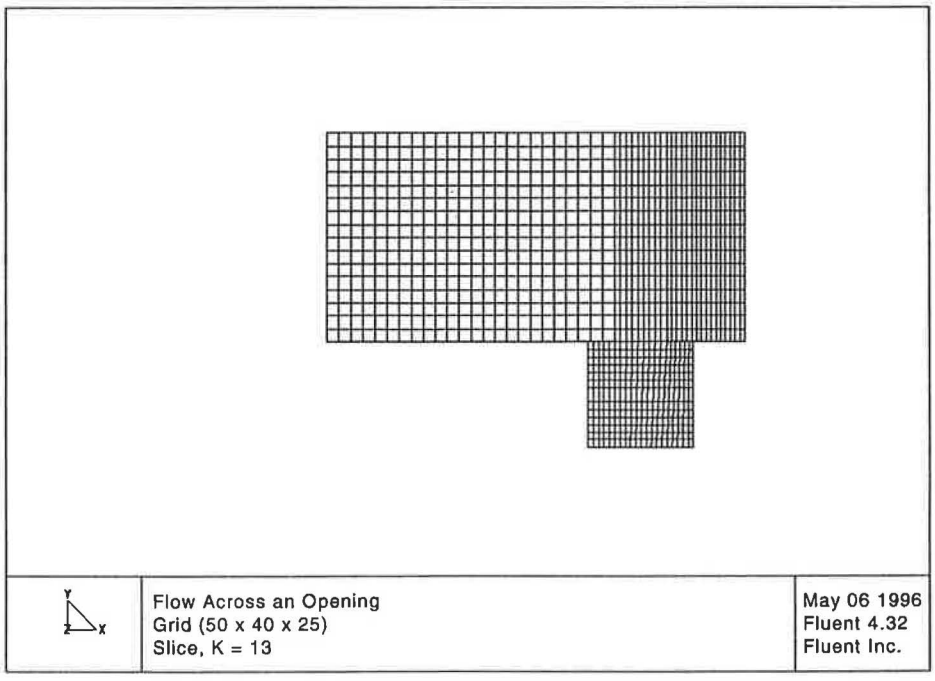

Fig. 2. Computational grid used for k–ϵ and Reynolds-stress models.

Reynolds stresses:

$$\rho\overline{u_i'u_i'} = \rho\frac{2}{3}k\partial_{ij} - \mu_t\left(\frac{\partial u_i}{\partial x_i} + \frac{\partial u_j}{\partial x_i}\right) + \frac{2}{3}\mu_t\frac{\partial u_1}{\partial x_1}\partial_{ij}. \quad (1)$$

k is the turbulent kinetic energy, given by

$$k = \tfrac{1}{2}\sum_i \overline{u_i^2}. \quad (2)$$

Equation (1) showing the Reynolds stresses is analogous to that describing the shear stresses in laminar flow, with the turbulent viscosity μ_t playing the same role as the molecular viscosity. The turbulent momentum equation now becomes

$$\mu_{eff} = \mu + \mu_t. \quad (3)$$

The turbulent viscosity μ_t is assumed to be proportional to turbulent velocity scale and length scale. In the k–ϵ model these velocity and length scales are obtained from the parameters k, the turbulent kinetic energy, and ϵ, the dissipation of k. The velocity scale is taken to be $k^{0.5}$, and the length scale is taken to be

$$\frac{k^{3/2}}{\epsilon}. \quad (4)$$

Hence, μ_t is given by

$$\mu_t = \rho C_u \frac{k^2}{\epsilon}, \quad (5)$$

where C_u is an empirical constant of proportionality. The values of k and ϵ are obtained by solution of the conservation equation.

RESULTS

Wind tunnel

The results from the air velocity transducer are shown in Fig. 3. Here we plot the velocity magnitude at various locations on three planes inside the box parallel to the wind direction. The planes are taken at one quarter, half, and three quarters of the box depth. The edges of the planes are 62.5 mm in from the vertical sides of the box since this was as close as the probe could be placed to the edges. The velocity magnitude is plotted as the height above the plane rather than plotting velocity contours. As we shall see later, this facilitates the comparison of wind tunnel and computational data. Also, the wind tunnel data have fewer points per section than the computational data and could introduce spurious contours due to measurement errors at any point. The orientation of the box can be deduced from the wind direction which is shown as a large arrow. From Fig. 3a, we see a large peak towards the back of the box which corresponds to the large eddy depicted in Fig. 1. Apart from this, there appears to be little variation across the box at this plane. Figure 3b also shows the effect of the large eddy in peaks towards the back of the box, and also at the front edge. Furthermore, there are other definite variations in velocity magnitude across the box which suggest the existence of smaller vortices. In particular, the two peaks in the front corners show secondary vortices. Figure 3c shows a similar picture where, in general, the higher velocity magnitudes are at the edges, whilst smaller peaks away from the extremities may correspond to less significant internal vortices.

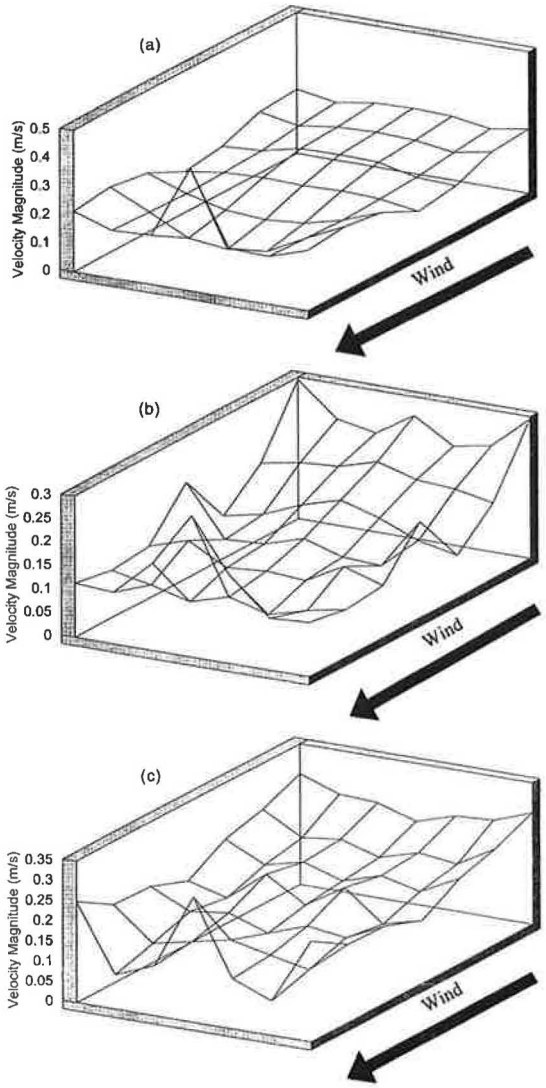

Fig. 3. Velocity magnitude on three horizontal planes inside the cube obtained from wind tunnel testing. All planes are 62.5 mm in from the vertical sides of the box. (a) Plane taken at one quarter depth. (b) Plane taken at half depth. (c) Plane taken at three quarters depth.

Figure 4 shows the velocity magnitudes at the opening. The plane chosen covers the entire physical opening. Here there is less spatial variation, with a gradual increase in velocity magnitude towards the back of the opening, but

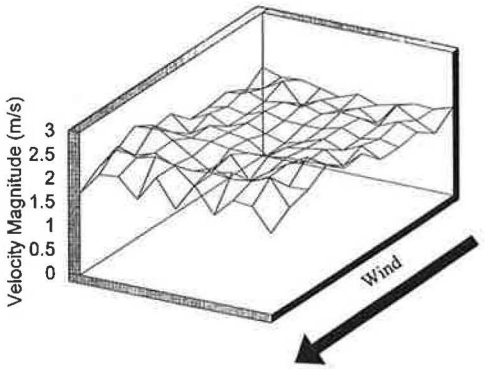

Fig. 4. Velocity magnitude at the opening obtained from wind tunnel testing.

there is considerable fluctuation of velocity magnitude at specific locations with time. However, the time constant of the probe tends to damp out these fluctuations, and we will only be concerned with the mean values. The time dependency of the flow at the opening is due to the smaller eddies of Fig. 1 which provide the mechanism for air exchange.

CFD: k–ϵ model

Figure 5a, b and c show the k–ϵ model CFD prediction of the velocity magnitude at the three planes inside the box. The edges of the planes were taken 62.5 mm in from the vertical sides of the box to allow exact comparison with the wind tunnel results of Fig. 3a, b and c. The first point to note is that the predicted values of velocity magnitude are much lower than the experimental results at every plane. Figure 5a does capture some of the influence of the large eddy with peaks at the front and back edge, but anticipates a much larger variation in velocity magnitude across the section. For Fig. 5b and c, at the middle and lower planes, whilst the general trend of higher values towards the edges is maintained, the predictions are much lower than the experimental results. Also the smaller internal vortices do not show up, and there is little variation in velocity magnitude across the sections. Figure 6 shows the k–ϵ CFD prediction of vel

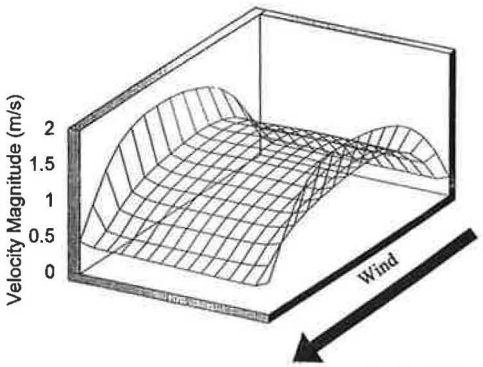

Fig. 6. Velocity magnitude at the opening obtained from the k–ϵ CFD model.

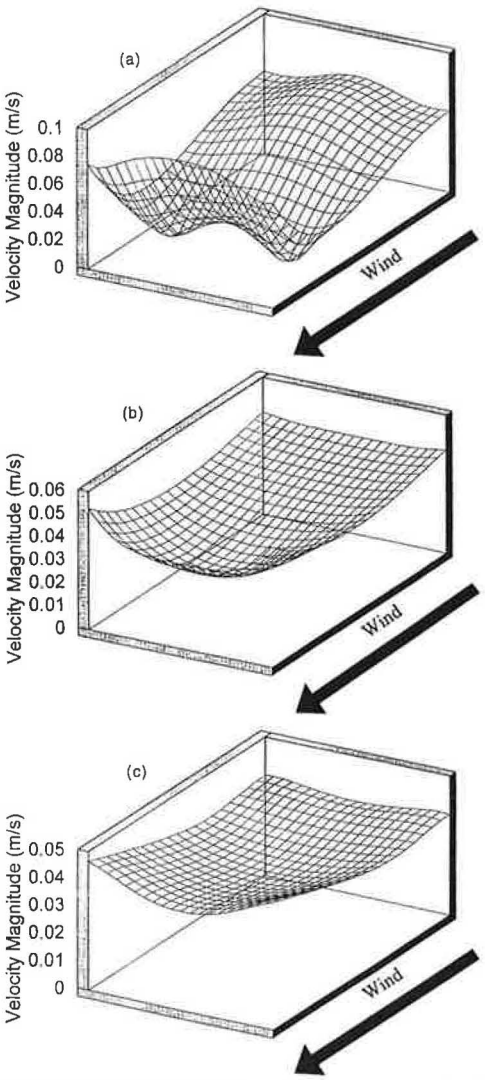

Fig. 5. Velocity magnitude on three horizontal planes inside the cube obtained from the k–ϵ CFD model. All planes are 62.5 mm in from the vertical sides of the box. (a) Plane taken at one quarter depth. (b) Plane taken at half depth. (c) Plane taken at three quarters depth.

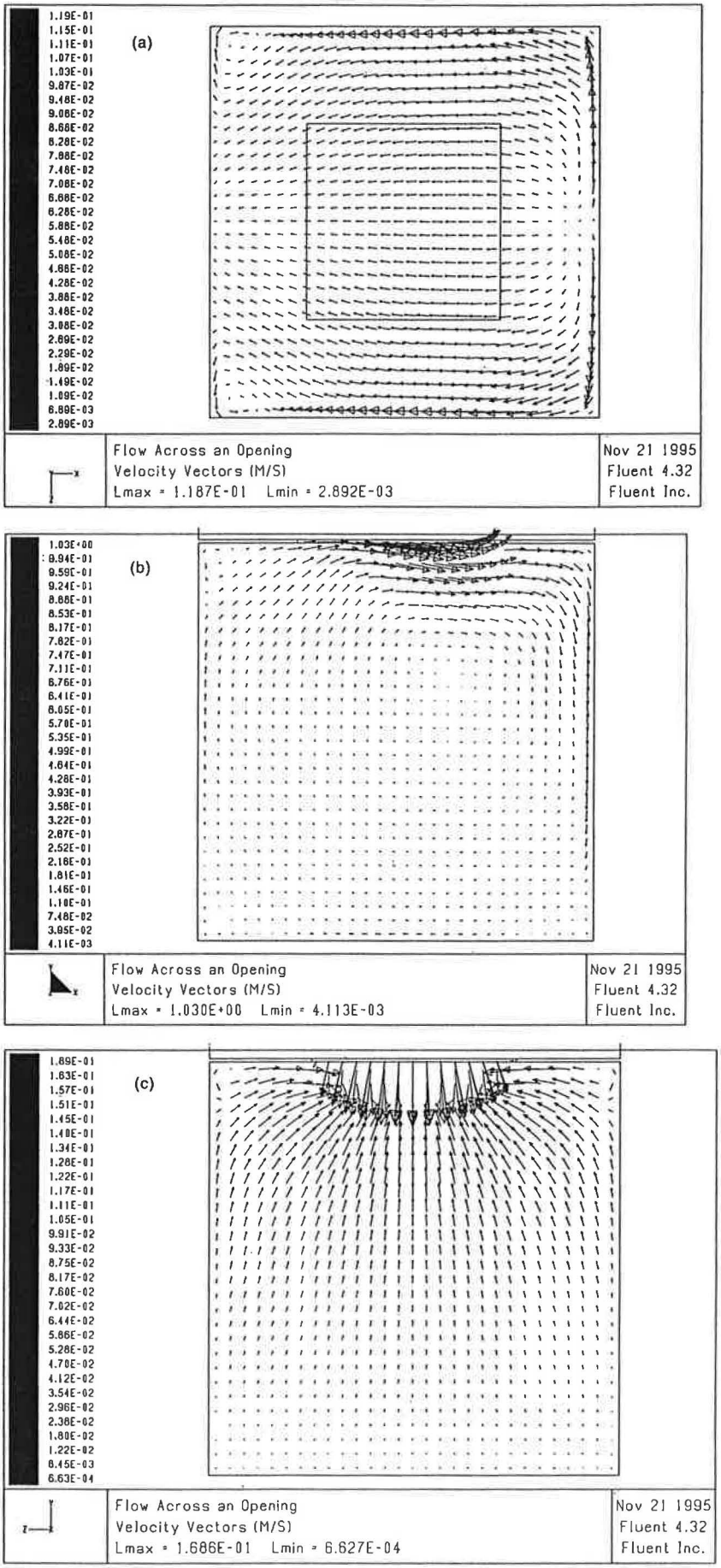

Fig. 7. The internal flow pattern predicted using the k–ϵ CFD model in the (a) xz, (b) xy and (c) yz planes.

ocity magnitude at the opening. The smooth velocity profile is in sharp contrast to the wind tunnel results of Fig. 4.

Figure 7a, b and c show the internal flow pattern predicted using the k–ϵ model in the xz, xy and yz planes respectively. These views correspond to looking from above, from the side, and at the plane perpendicular to the wind direction. Figure 7a shows the flow travelling from right to left across the top of the box, with some secondary flow depicted in the bottom left-hand and top left-hand corners. Figure 7b shows some flow entering and leaving the box at the opening, and a large internal flow. However, this internal flow is much weaker than the wind tunnel results predicted. Figure 7c shows flow entering the box through the opening. As a whole, the computational model depicts the large vortex qualitatively, but shows almost no secondary flow.

CFD: Reynolds-stress model

Figure 8a, b and c show the Reynolds-stress model prediction of the velocity magnitude at the three planes inside the box taken 62.5 mm in from the vertical sides of the box. These should be compared with the wind tunn data (Fig. 3a, b and c), and the k–ϵ model results (F 5a, b and c). In general, the Reynolds-stress predictio are much more encouraging than the k–ϵ model in th many of the trends in the wind tunnel data that the k model ignored are preserved. Also, the data are of simil magnitude. Figure 8a predicts a slightly smaller peak velocity magnitude towards the back of the box than t wind tunnel data, but also detects the much smaller pea in the back corners of the box. Figure 8b is most encou aging in that the five peaks in the wind tunnel data a all predicted with reasonable accuracy. Figure 8c aga is a good qualitative result, but shows greater spat variation and higher peaks than the wind tunnel da suggest.

The resultant flow patterns are shown in Fig. 9a, b a c in the xz, xy and yz planes respectively. These vie correspond to looking from above, from the side, and the plane perpendicular to the wind direction. Whilst t x–y projection (Fig. 9b) shows little detail except for t large eddy, the x–z and y–z projections (Fig. 9a and respectively) show that there are significant seconda

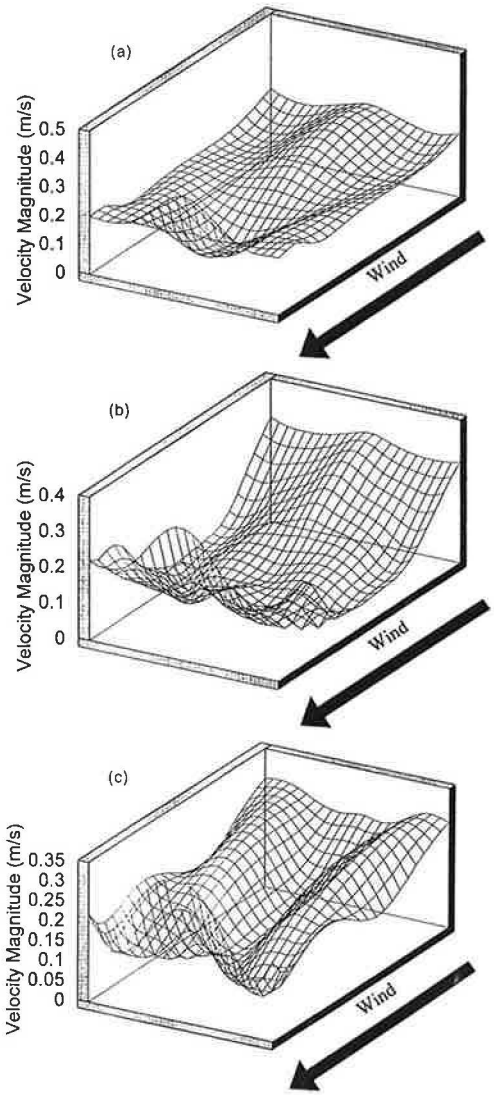

Fig. 8. Velocity magnitude on three horizontal planes inside the cube obtained from the Reynolds-stress CFD model. All planes are 62.5 mm in from the vertical sides of the box. (a) Plane taken at one quarter depth. (b) Plane taken at half depth. (c) Plane taken at three quarters depth.

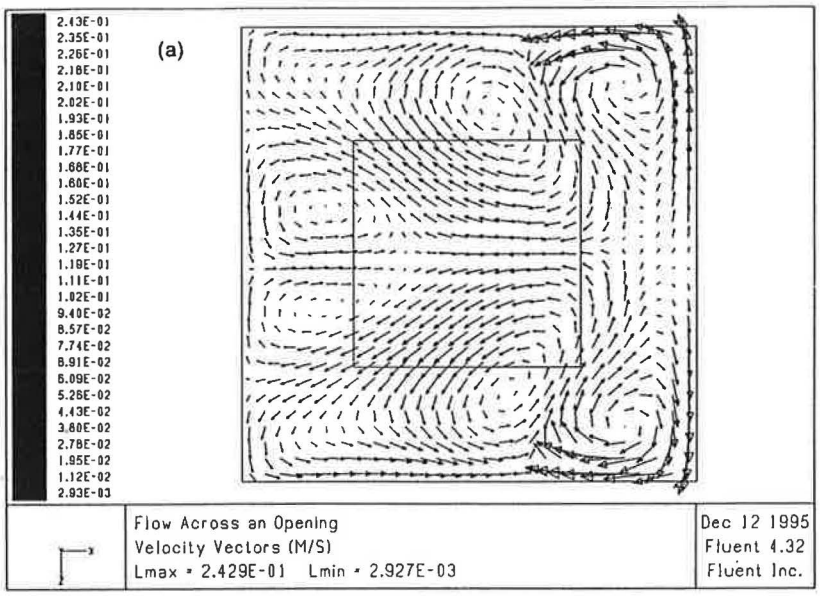

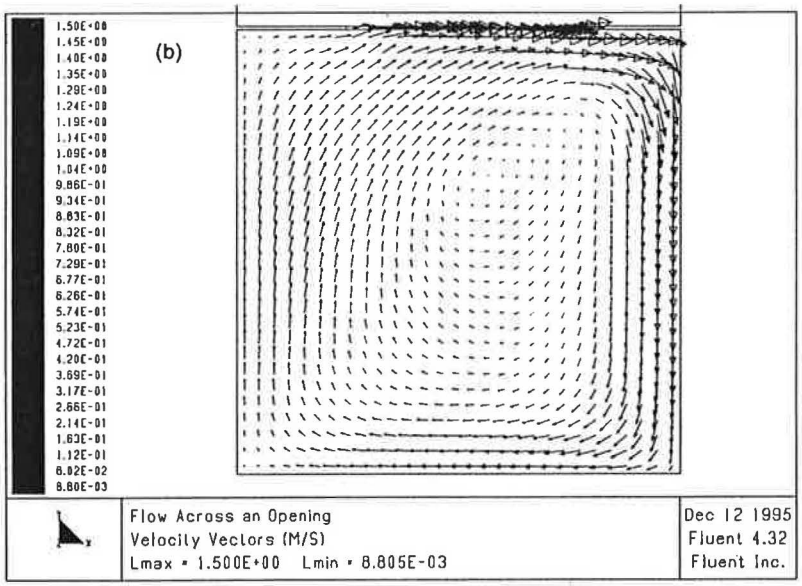

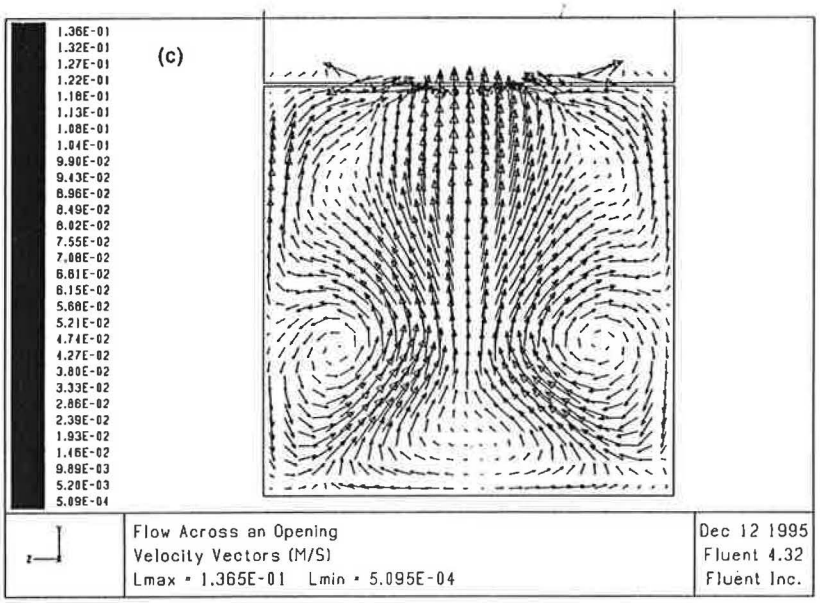

Fig. 9. Internal flow pattern predicted using the Reynolds-stress CFD model in the (a) *xz*, (b) *xy* and (c) *yz* planes respectively.